Tuning Tailored Single-Walled Carbon Nanotubes by Highly Energetic Heavy Ions

Ayman S. El-Said,[1,*] Saleem Rao,[1] Shavkat Akhmadaliev,[2] and Stefan Facsko[2]

[1] *Physics Department, King Fahd University of Petroleum and Minerals, Dhahran 31261, Saudi Arabia*

[2] *Institute of Ion Beam Physics and Materials Research, Helmholtz-Zentrum Dresden-Rossendorf, 01328 Dresden, Germany*

(Received 15 October 2019; revised manuscript received 19 March 2020; accepted 14 April 2020; published 28 April 2020; corrected 22 May 2020)

Carbon-based nanomaterials have attracted a lot of interest lately due to their highly promising applications. Here we report on the modifications of single-walled carbon nanotubes (SWCNTs) induced by swift (highly energetic) heavy ions. Using scanning force microscopy and Raman spectroscopy, we observe a dramatic change in the structure of the irradiated SWCNTs, accompanied by an increase of the adhesion force as a function of ion fluence and electronic energy loss. With increasing ion fluence, the SWCNTs exhibit a partial transformation from metallic to more semiconducting. Moreover, at high fluence they break into segments 10–20 nm long.

DOI: 10.1103/PhysRevApplied.13.044073

I. INTRODUCTION

Highly energetic heavy ions have become an important tool for modifying various materials for a wide range of applications in the last two decades [1,2]. This is mainly due to the high-energy deposition in a small volume along the ion track. On the basis of the material type and the ion-beam parameters, various swift-heavy-ion-induced modifications are created not only in the structure but also in the mechanical, electronic, and magnetic properties of the irradiated materials. Among the samples investigated, nanomaterials, such as carbon nanotubes (CNTs) and in particular semiconducting single-walled carbon nanotubes (SWCNTs), are the most-promising one-dimensional electronic materials, with exceptional properties such as high mobility on the order of 100 000 $cm^2/V\,s$, [1–3] current densities of more than 10^9 A/cm^2, and *on*:*off* current ratios exceeding 10^5. These remarkable properties led to a wide range of applications in contemporary technologies, such as CNT-based FETs, biological sensors, drug delivery, and energy storage [4–6]. In addition, SWCNTs have been explored as promising materials for electromagnetic interference shielding, which is very important for electronic devices, such as laptops, cell phones, weather radars, and TV-picture transmitters, and in particular in space applications [7]. One might expect that ion irradiation should have the same effects on nanomaterials as on solid materials. However, it has recently been demonstrated that ion irradiation can induce interesting effects on nanostructured materials. Examples include structural engineering of two-dimensional materials, nanofabrication of quantum dots, and self-assembly or self-organization in carbon nanosystems [8–10]. Controlling the modifications induced in SWCNTs is vital for tuning their mechanical, electrical, and optical properties, as they strongly depend on the chirality and defects present [11,12]. It was demonstrated that the atomic structure and morphology of CNTs or related structures can be modified by ion irradiation [13,14]. They can even be interconnected or merged in a controllable way [15,16]. Although ion irradiation of materials usually introduces disorder or defects, recent experiments concerning ion irradiation of various nanostructures demonstrated that it could provide unique effects [17–19]. Defect healing that can lead to useful localized modification has been reported under controlled heavy-ion irradiation in carbon nanotubes [19–21]. Another important aspect is the presence of fast heavy ions in the space environment, which makes studying their effects on the physical properties of SWCNTs essential for all possible space applications using SWCNTs. Here we present irradiation experiments on SWCNTs using highly energetic heavy ions in which the structure and the associated adhesion force are modified in a controlled way by our simply tuning the ion fluence and the kinetic energy of the swift heavy ions.

II. EXPERIMENTAL DETAILS

Our experiments start with sample preparation by our immersing precleaned commercially available silicon substrates in a solution of SWCNTs in dichlorobenzene (0.03 mg/ml) for 3 min. CVD-grown SWCNTs, 1 nm

*elsaid@kfupm.edu.sa

TABLE I. Parameters of the iodine ions used for irradiation of SWCNTs [kinetic energy (E_{kin}), ion fluence (φ), electronic stopping $(dE/dx)_e$, nuclear stopping $(dE/dx)_n$, mean range (R)] calculated with SRIM-2013.

Ions	E_{kin} (MeV)	$(dE/dx)_e$ (keV/nm)	$(dE/dx)_n$ (keV/nm)	R (μm)	φ (cm^{-2})
I^{5+}	20	6.03	0.30	5.11	5×10^{13}–10^{15}
I^{6+}	30	8.14	0.22	6.46	5×10^{12}–10^{15}
I^{9+}	54	11.4	0.14	8.84	5×10^{13}

in diameter, are obtained from Sigma-Aldrich. After the SWCNTs have been placed in dichlorobenzene, the mixture is sonicated for 10 min to obtain a homogeneous suspension of SWCNTs in the solvent. The solution of SWCNTs is then sonicated for 1 min just before the silicon substrate is dipped in it. After removal of the substrate from the SWCNT solution, it is dried under ambient conditions without any rinsing. All samples are prepared from the same solution of SWCNTs following the same procedure. After preparation, the samples are irradiated at room temperature with swift iodine ions of various megaelectronvolt kinetic energies and fluences from the 6-MV Tandetron at Helmholtz-Zentrum Dresden-Rossendorf (Dresden, Germany). The ion-irradiated samples are inspected with a Bruker Nanoscope III scanning force microscope (SFM). The microscope is operated in PeakForce Tapping mode under ambient conditions with use of Bruker probe of 1.5 nN spring constant. This mode is based mainly on the acquisition of force-distance curves at each pixel, which allows the mapping of the elastic properties of the surface investigated. The image processing and analysis of SFM topographic images are performed with the software program WSxM (version 5.0 Develop 6.4) from Nanotec Electronica [22]. In addition, Raman spectroscopy is performed to identify the induced defects in the irradiated SWCNTs.

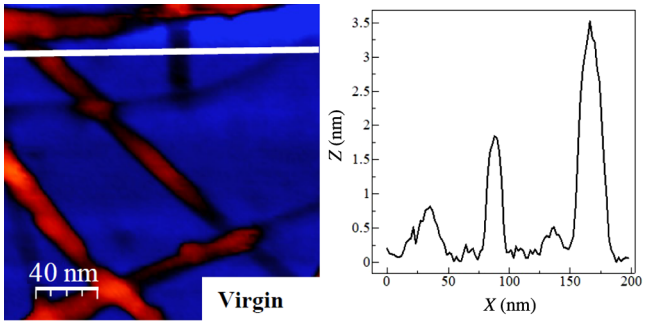

FIG. 1. Topographic SFM image and line profiles for SWCNTs on Si substrate.

III. RESULTS AND DISCUSSION

The energy deposition of swift heavy ions in materials proceeds via two channels: the electronic energy loss due to the interaction with the electronic system of the material and the nuclear energy loss transferring the ion energy to the target atoms via elastic collisions with the nuclei. For the high kinetic energies up to 54 MeV used in our experiments, the electronic energy loss dominates and consequently strong electronic excitations and ionizations along the ion track are induced. The ion species used and the corresponding parameters, as calculated by SRIM-2013 [23], are listed in Table I.

The SFM topographic images in Figs. 1, 2, 3(a)–3(c), and 3(g)–3(i) show the virgin and irradiated samples with SWCNTs and their bundles of different sizes lying on the

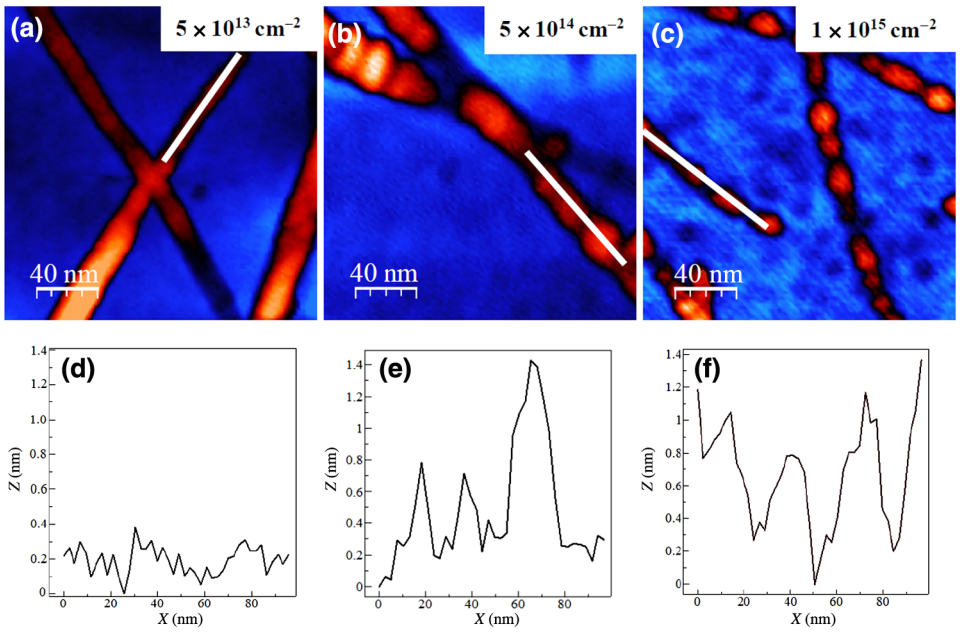

FIG. 2. Topographic SFM images [(a)–(c)] and line profiles [(d)–(e)] for SWCNTs irradiated with 30-MeV iodine ions of various ion fluences.

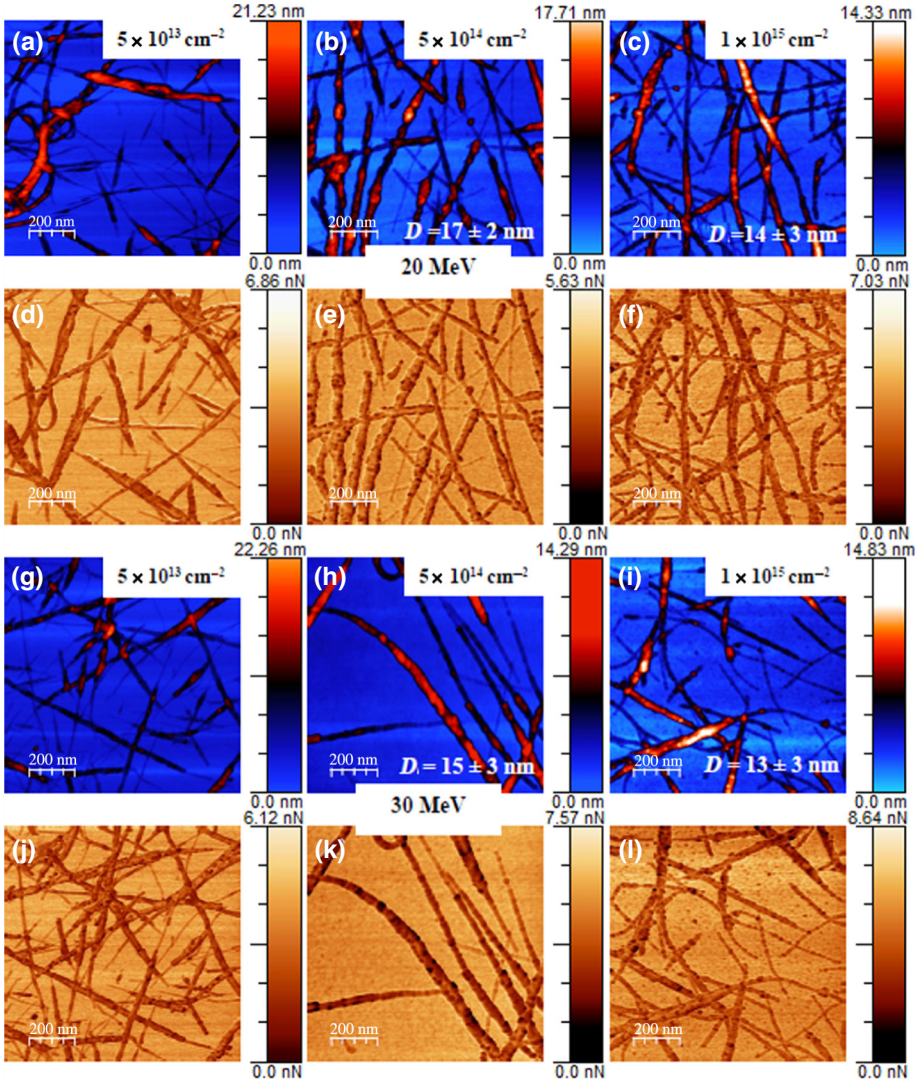

FIG. 3. Topographic SFM [(a)–(c),(g)–(i)] adhesion-force-mapping [(d)–(f),(j)–(l)] images of SWCNTs irradiated with 20- and 30 MeV iodine ions of various ion fluences. The average size (D) of the broken segments is shown.

surface of Si substrates. Furthermore, the SFM images and the corresponding line profiles show clear deformation of the ion-irradiated tubes and their bundles into broken segments at high ion fluence. Moreover, the segments become smaller as the ion fluence increases, as shown in Fig. 2. In addition to the measured topographic images, adhesion-force mapping is performed simultaneously in PeakForce Tapping mode, giving the possibility to determine the adhesion force between the tip and the tubes and the substrate. In this way, high-resolution images are acquired with detailed features, including the broken segments, of the ion-irradiated SWCNTs, as shown in Figs. 3(d)–3(f) and 3(j)–3(l). Figure 4 shows the distributions of the adhesion force extracted from 1000×1000 nm^2 adhesion-force images for SWCNTs irradiated with ion fluences of 5×10^{13}–10^{15} and kinetic energies of 20, 30, and 54 MeV. While the high peaks of the histograms in Fig. 4 correspond to the substrates, the broad peak at smaller adhesion force represents the SWCNTs. The mean values of the adhesion forces are determined by our fitting a Gaussian function to each histogram for the SWCNTs. The mean values of the adhesion force increase as a function of ion fluence from 2.2 ± 0.6 nN at $\varphi = 5 \times 10^{13}$ cm^{-2} to 4.0 ± 0.5 nN at $\varphi = 1 \times 10^{15}$ cm^{-2} for 30-MeV I ions. Only a slight increase of the adhesion force as a function of electronic energy loss $(dE/dx)_e$ for the iodine ions used is observed, as shown in Figs. 4(e)–4(g). It is worthwhile mentioning that ion irradiation may lead to a change of adhesion of the substrate. However, consider only the response of SWCNTs to ion irradiation.

The most-prominent peaks in the measured Raman spectra are the disorder peak (D peak), which is an indication of the presence of defects in SWCNTs, and the G peak originating from longitudinal optical phonons. In SWCNTs, the G band is split into two peaks, the G^- and G^+ peaks (see Fig. 5), which originate from the longitudinal optical modes in metallic and semiconducting nanotubes, respectively[24,25]. The high-intensity and narrow

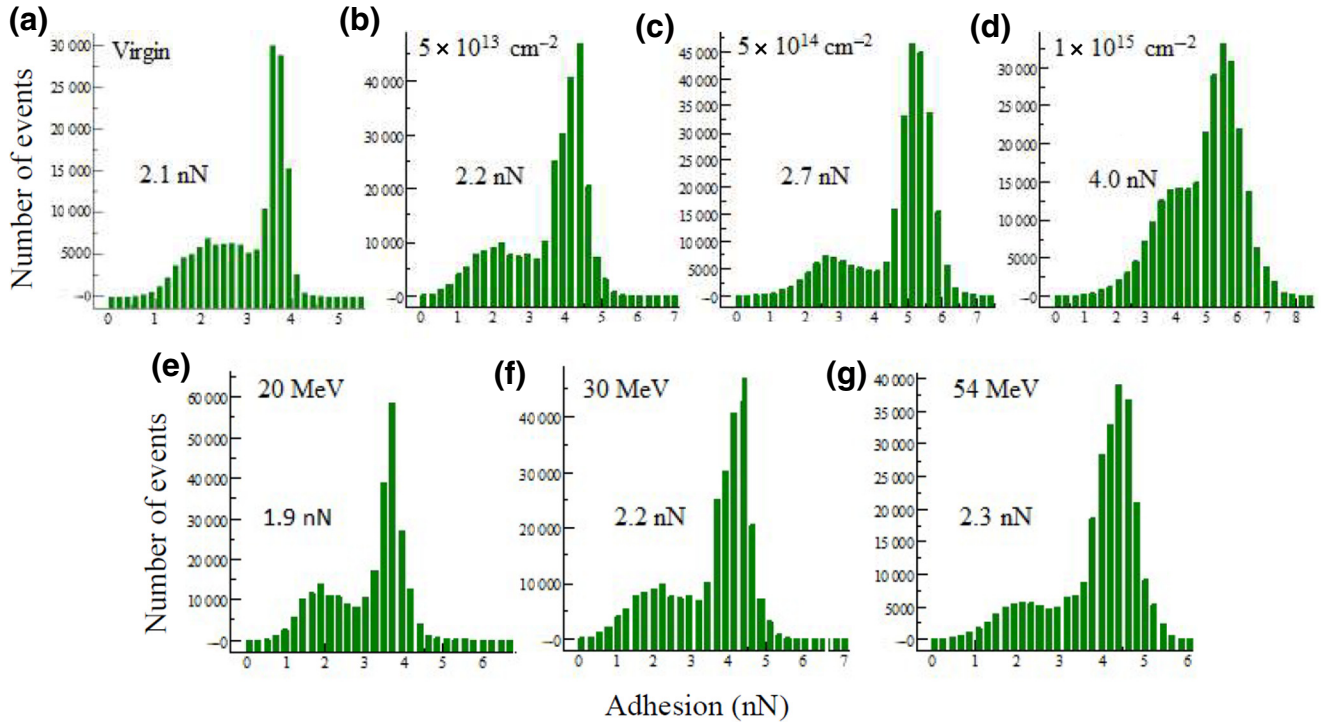

FIG. 4. (a)–(d) Frequency distribution of adhesion force for virgin SWCNTs on Si substrates and irradiated with 30-MeV iodine ions of various ion fluences. (e)–(g) Histograms for SWCNTs irradiated with 5×10^{13} I ions/cm^2 of different kinetic energies. The mean adhesion force of SWCNTs is shown.

profile of the G^+ peak in comparison with the broad G^- peak indicates that our virgin SWCNTs are more metallic. This reduction of the intensity and broadening of the G^- peak is mainly caused by the existence of electron-phonon coupling in metallic nanotubes [25,26]. However, on increase of the ion fluence, the Raman spectra show a gradual change in the asymmetric G^- peak and the initially sharp G^+ peak, which can be ascribed to the partial transformation from metallic to semiconducting SWCNTs, as shown in Fig. 5. In addition, we observe a greater reduction in the intensity of the G^- peak in comparison with the G^+ peak for ions with higher $(dE/dx)_e$. Furthermore, we observe that the G^+ peak becomes relatively wider on increase of $(dE/dx)_e$ at the same ion fluence; see Fig. 6. This indicates that more defects are created in the SWCNTs. This is demonstrated by our observing an increase of the disorder parameter (I_D/I_G) as a function of ion fluence, as shown in Fig. 7.

I_D/I_G increases as a function of φ until it saturates at $\varphi = 5 \times 10^{13}$ cm^{-2}, reaching a slightly smaller value at $\varphi = 1 \times 10^{15}$ cm^{-2}, which is an indication of defect healing, as demonstrated in previous experiments using different ion species and kinetic energies [20,21]. Furthermore, it is also possible that ion-induced amorphization occurs at high ion fluence [27]. This can be seen also form the deformation of the irradiated nanotubes.

Another parameter extracted from the measured Raman spectra, with use of the Tuinstra-Koenig relation, is the crystallite size (L_d) [28], which is also termed the "interdefect length" (L_d), using the Tuinstra-Koenig relation [29–32]. In contrast to I_D/I_G, L_d decreases as a function of φ, which is ascribed to the creation of more defects on increase of ion fluence, as depicted in Fig. 7. Therefore, a greater value of the disorder parameter and consequently a shorter interdefect length are observed at high fluence, where the SWCNTs are drastically damaged, leading to breaking of the nanotubes into undamaged segments of length L_d. This agrees with the SFM observations

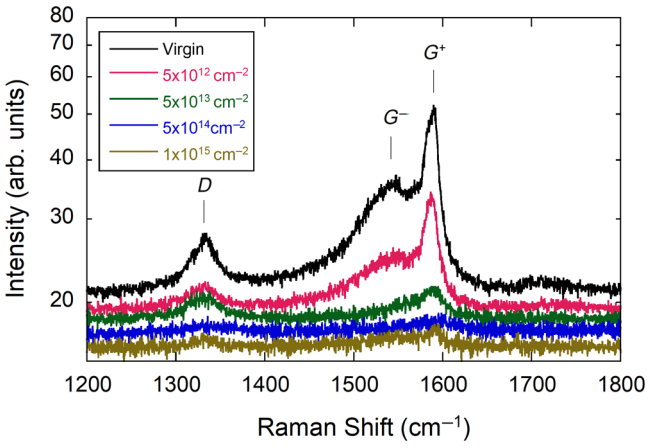

FIG. 5. Raman spectra of SWCNTs irradiated with 30 MeV I of different fluencies.

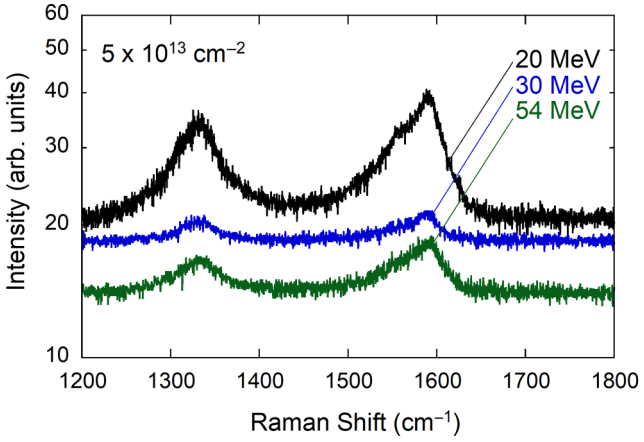

FIG. 6. Raman spectra of SWCNs irradiated with 5×10^{13} I ions/cm^2 of different kinetic energies.

of broken segments (D), which become smaller at higher ion fluence. Moreover, the size of the broken segments is estimated from the SFM images to be 10–20 nm, which is in fair agreement with the estimated L_d values, as shown in Figs. 2 and 7.

However, fragmentation of the nanotubes is observed after $\varphi = 5 \times 10^{13}$ cm^{-2} is passed, which coincides with the fluence at which the saturation of the disorder parameter of SWCNTs occurs. The defects responsible for these effects are created by the coupling of the electron excitation induced by the megaelectronvolt ions to the phononic system. In the concept of the thermal-spike model, the electron-phonon coupling leads to a temperature increase in the irradiated zone, which causes structural modifications [33,34]. In addition, the observed modifications of SWCNTs are in agreement with the results of classical molecular-dynamics simulations, which have shown that irradiation with high ion fluence can lead to the breakup of nanotubes, amorphization, and partial or total loss of the tubular shape [27].

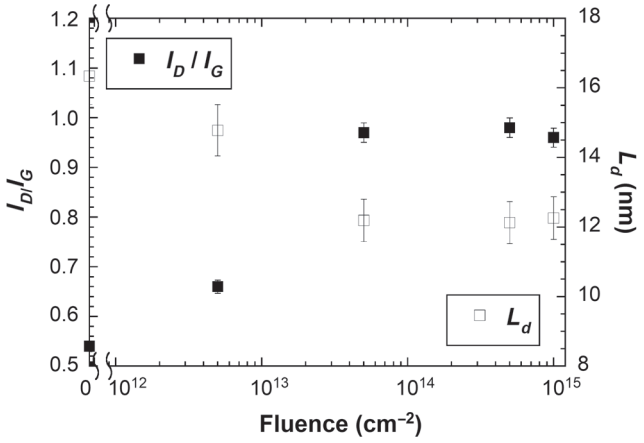

FIG. 7. Disorder parameter (I_D/I_G) and interdefect length (L_d) as a function of ion fluence.

IV. CONCLUSIONS

We show that swift heavy ions are able to modify single-walled carbon nanotubes in a controlled way. Ion-induced fragmentation of broken segments is observed as a function of ion fluence. The segments are observed only after an ion-fluence threshold of 5×10^{13} cm^{-2} is passed, which coincides with the fluence at which the disorder parameter measured by Raman spectroscopy saturates. In addition, we demonstrate that the adhesion between the SFM probe and SWCNTs can be changed significantly by varying the ion fluence, and slightly by varying the electronic energy loss of the ions used.

ACKNOWLEDGMENTS

A.S.E. acknowledges the support of King Fahd University of Petroleum and Minerals (Project No. ISSP1801). The assistance of A. Keller in PeakForce Tapping measurements is appreciated. Parts of this research were performed at the Ion Beam Center of Helmholtz-Zentrum Dresden-Rossendorf, a member of the Helmholtz Association.

[1] F. Aumayr, S. Facsko, A. S. El-Said, C. Trautmann, and M. Schleberger, Single-ion induced surface nanostructures: A comparison between slow highly-charged and swift heavy ions, J. Phys.: Condens. Matter **23**, 393001 (2011).

[2] A. Javey, G. Guo, Q. Wang, M. Lundstrom, and H. J. Dai, Ballistic carbon nanotube field-effect transistors, Nature **424**, 654 (2003).

[3] S. J. Tans, A. R. M. Verschueren, and C. Dekker, Room-temperature transistor based on a single carbon nanotube, Nature **393**, 49 (1998).

[4] F. L. Michael, D. Volder, S. H. Tawfick, R. H. Baughman, and A. J. Hart, Carbon nanotubes: Present and future commercial applications, Science **339**, 535 (2013).

[5] G. Wu, P. Tan, D. Wang, Z. Li, L. Peng, Y. Hu, C. Wang, W. Zhu, S. Chen, and W. Chen, High-performance supercapacitors based on electrochemical-induced vertical-aligned carbon nanotubes and polyaniline nanocomposite electrodes, Sci. Rep. **7**, 43676 (2017).

[6] W. Kwak, K. Lau, C. Shin, K. Amine, L. A. Curtiss, and Y. Sun, A Mo2C/carbon nanotube composite cathode for lithium-oxygen batteries with high energy efficiency and long cycle life, ACS Nano **9**, 4129 (2015).

[7] L. Cai and C. Wang, Carbon nanotube flexible and stretchable electronics, Nanoscale Res. Lett. **10**, 320 (2015).

[8] A. V. Krasheninnikov and F. Banhart, Engineering of nanostructured carbon materials with electron or ion beams, Nat. Mater. **6**, 723 (2007).

[9] E. Trynkiewicz, B. R. Jany, A. Janas, and F. Krok, Recent developments in ion beam-induced nanostructures on AIII-BV compound semiconductors, Phys. Condens. Matter **30**, 304005 (2009).

[10] Z. Li and F. Chena, Ion beam modification of two-dimensional materials: Characterization, properties, and applications, Appl. Phys. Rev. **4**, 011103 (2017).

[11] Y.-H. Kim, J. Choi, K. Chang, and D. Tománek, Defective fullerenes and nanotubes as molecular magnets: An ab initio study, Phys. Rev. B **68**, 125420 (2003).
[12] M. Y. Han, B. Zyilmaz, Y. Zhang, and P. Kim, Energy Band-Gap Engineering of Graphene Nanoribbons, Phys. Rev. Lett. **98**, 206805 (2007).
[13] D. Ugarte, Curling and closure of graphitic networks under electron-beam irradiation, Nature **359**, 707 (1992).
[14] A. Kis, G. Csányi, J.-P. Salvetat, Thien-Nga Lee, E. Couteau, A. J. Kulik, W. Benoit, J. Brugger, and L. Forró, Reinforcement of single-walled carbon nanotube bundles by intertube bridging, Nat. Mater. **3**, 153 (2004).
[15] M. Terrones, H. Terrones, F. Banhart, J. Charlier, and P. M. Ajayan, Coalescence of single-walled carbon nanotubes, Science **288**, 1226 (2000).
[16] M. Terrones, F. Banhart, N. Grobert, J.-C. Charlier, H. Terrones, and P. M. Ajayan, Molecular Junctions by Joining Single-Walled Carbon Nanotubes, Phys. Rev. Lett. **89**, 075505 (2002).
[17] A. V. Krasheninnikov and K. Nordlund, Ion and electron irradiation-induced effects in nanostructured materials, J. Appl. Phys. **107**, 071301 (2010).
[18] M. C. Ridgway, F. Djurabekova, and K. Nordlund, Ion-solid interactions at the extremes of electronic energy loss: Examples for amorphous semiconductors and embedded nanostructures, Solid State Mater. Sci. **19**, 29 (2015).
[19] D. K. Avasthi, Y. K. Mishra, F. Singh, and J. P. Stoquert, Ion tracks in silica for engineering the embedded nanoparticles, Nucl. Instrum. Methods B **268**, 3027 (2010).
[20] A. Kumar, D. K. Avasthi, J. C. Pivin, and P. M. Koinkar, Ordering of fullerene and carbon nanotube thin films under energetic ion impact, Appl. Phys. Lett. **92**, 221904 (2008).
[21] A. V. Krasheninnikov and K. Nordlund, Irradiation effects in carbon nanotubes, Nucl. Instrum. Methods B **216**, 355 (2004).
[22] I. Horcas, R. Fernández, J. M. Gómez-Rodríguez, J. Colchero, J. Gómez-Herrero, and A. M. Baro, WSXM: A software for scanning probe microscopy and a tool for nanotechnology, Rev. Sci. Instrum. **78**, 013705 (2007).
[23] J. F. Ziegler, M. D. Ziegler, and J. P. Biersack, SRIM – the stopping and range of ions in matter (2010), Nucl. Instrum. Methods B **268**, 1818 (2010).
[24] K. Kempa, Gapless plasmons in carbon nanotubes and their interactions with phonons, Phys. Rev. B **66**, 195406 (2002).
[25] H. Telg, M. Fouquet, J. Maultzsch, Y. Wu, B. Chandra, J. Hone, T. F. Heinz, and C. Thomsen, G− and G+ in the Raman spectrum of isolated nanotube: A study on resonance conditions and lineshape, Phys. Status Sol. (b) **245**, 2189 (2008).
[26] R. Krupke, F. Hennrich, H. Löhneysen, and M. M. Kappes, Separation of metallic from semiconducting single-walled carbon nanotubes, Science **301**, 344 (2003).
[27] A. V. Krasheninnikov, K. Nordlund, J. Keinonen, and F. Banhart, Ion-irradiation-induced welding of carbon nanotubes, Phys. Rev. B **66**, 245403 (2002).
[28] F. Tuinstra and J. L. Koenig, Raman spectrum of graphite, J. Chem. Phys. **53**, 1126 (1970).
[29] M. M. Lucchese, F. Stavale, E. H. M. Ferreira, C. Vilani, M. V. O. Moutinho, R. B. Capaz, C. A. Achete, and A. Jorio, Quantifying ion-induced defects and Raman relaxation length in graphene, Carbon **48**, 1592 (2010).
[30] Vishalli, D. K. Avasthi, A. Srivastava, and K. Dharamvir, Transformation of multi walled carbon nanotubes irradiated by swift heavy ions, Nucl. Instrum. Methods B **407**, 172 (2017).
[31] A. Olejniczak and V. A. Skuratov, Effect of swift heavy ion irradiation on single-and multiwalled carbon nanotubes, Nucl. Instrum. Methods B **326**, 33 (2014).
[32] L. G Canado, A. Jorio, and M. A. Pimenta, Measuring the absolute Raman cross section of nanographites as a function of laser energy and crystallite size, Phys. Rev. B **76**, 064304 (2007).
[33] C. Dufour, V. Khomrenkov, Y. Y. Wang, F. Aumayr, and M. Toulemonde, An attempt to apply the inelastic thermal spike model to surface modifications of CaF_2 induced by highly charged ions: Comparison to swift heavy ions effects and extension to some others material, J. Phys: Condens. Matter **29**, 095001 (2017).
[34] A. S. El-Said, R. A. Wilhelm, R. Heller, M. Sorokin, S. Facsko, and F. Aumayr, Tuning the Fabrication of Nanostructures by Low-Energy Highly Charged Ions, Phys. Rev. Lett. **117**, 126101 (2016).

Correction: The previously published Figure 3(a) was converted improperly during the production cycle and has now been rendered optimally.